Modelling of Breakdown Voltage and Its Temperature Dependence in SAGCM InP/InGaAs Avalanche Photodiodes

C. L. F. Ma, M. J. Deen, L. E. Tarof*, J. Yu*

School of Engineering Science, Simon Fraser University, Burnaby, British Columbia, V5A 1S6 Canada

*Bell-Northern Research Ltd., P. O. Box 3511, Station C, Ottawa, Ontario K1Y 4H7 Canada

Abstract

We investigate breakdown voltage and its temperature dependence from -40 °C to 110 °C in SAGCM InP/InGaAs avalanche photodiodes. The experimental data shows that the breakdown voltage is approximately a linear function of temperature, with a temperature coefficient η between 0.14 to 0.18 V/°C, and this η is in agreement with our physical model. The successful application of the physical model implies that the empirical formula used here for temperature dependence of the impact ionization coefficients in InP is verified.

Introduction

Separate absorption, grading, charge, and multiplication (SAGCM) InP/InGaAs avalanche photodiode (APD) offers many attractive features as a high-performance photodetector for today's long distance, high-bit-rate fiber optical telecommunication systems [1-3]. However, since the first successful fabrication of planar SAGCM InP/InGaAs APDs with partial charge sheet in the device periphery [1] (Fig.1 with device parameters in Table 1), there has not been any detailed modelling of their electrical or optical characteristics. Here, we will investigate the breakdown voltage V_{br} and its temperature dependence. This work represents, for the first time, an attempt to theoretically investigate the temperature dependence of breakdown voltage in any type of InP-based APDs.

Room temperature V_{br}

If all the device parameters are known, V_{br} at room temperature can be theoretically calculated. However, in practice, two critical device parameters - the multiplication layer thickness x_d and charge sheet density σ_{charge}, vary significantly over a wafer using existing MOCVD fabrication. Presently, existing techniques for measuring these two device parameters, such as secondary ion mass spectroscopy (SIMS) and Hall analysis (C-V measurement has not been successful due to APDs' small size and complex geometry), are destructive and/or require calibration wafers, and more importantly, the accuracy of these measurements make it impossible to predict V_{br} better than ±5 V. These two device parameters are extracted [4], using experimental V_{mesa} (as defined soon) and V_{br} at room temperature.

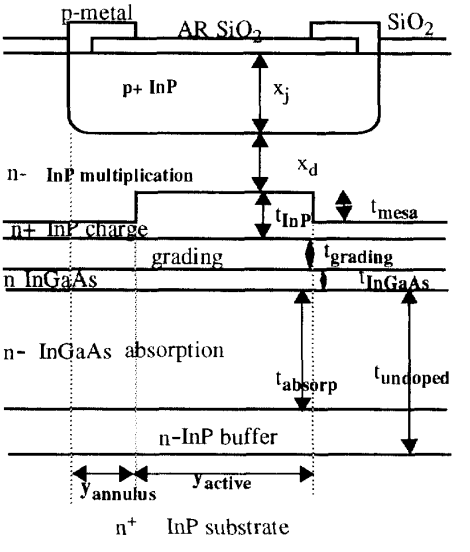

Fig. 1 Planar SAGCM InP/InGaAs APD with partial charge sheet in the device periphery.

Table 1 Nominal device parameters for the SAGCM APDs.

y_{active}	30 μm	$y_{annulus}$	5 μm
t_{mesa}	0.11μm	x_j	2.2 μm
t_{InP}	0.17 μm	$t_{undoped}$	3.8 μm
$t_{grading}$, N_G	0.09 μm, ~10^{16}cm^{-3}	t_{absorp}	2.8 μm
t_{InGaAs}, N_{InGaAs}	0.02 μm, 2×10^{17}cm^{-3}	n^--InP, n^--InGaAs	10^{15}cm^{-3}

A typical dark current and photo current versus bias voltages are shown in Fig. 2. All properly designed APDs including SAGCM InP/InGaAs APDs show impact ionization breakdown at some voltage V_{br}. However, an additional characteristic voltage in SAGCM InP/InGaAs APDs, which can be unambiguously determined from photocurrent-voltage characteristics (Fig. 2) [1], is the punchthrough voltage V_{mesa}, at which the electric field starts to penetrate the InGaAs layers. With these two

0-7803-2111-1 $4.00 © 1994 IEEE

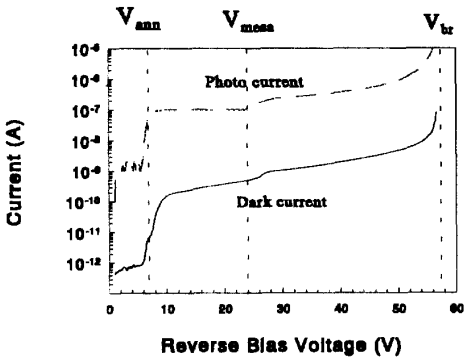

Fig. 2 A typical (APD32) DC characteristics of SAGCM InP/InGaAs APD at λ=1.3μm.

experimental voltages, two device parameters may be extracted, for examples, x_d and σ_{charge} [4]. Defining F_{br} as the electric field in the multiplication layer at breakdown, we get

$$V_{mesa} = \frac{q\sigma_{charge}}{\varepsilon_1\varepsilon_0}\left(x_d + \frac{t_{InP}}{2}\right) + \frac{qN_G t_{grading}}{\varepsilon_2\varepsilon_0}\left(x_d + t_{InP} + \frac{t_{grading}}{2}\right), \quad (1)$$

$$V_{br} = F_{br}(x_d + t_{InP} + t_{grading} + t_{undoped}) - \frac{q\sigma_{charge}}{\varepsilon_1\varepsilon_0}\left(\frac{t_{InP}}{2} + t_{grading} + t_{undoped}\right) - \frac{qN_G t_{grading}}{\varepsilon_2\varepsilon_0}\left(\frac{t_{grading}}{2} + t_{undoped}\right) - \frac{q\sigma_{InGaAs}}{\varepsilon_2\varepsilon_0}t_{undoped} - \frac{qN_D}{2\varepsilon_2\varepsilon_0}t_{undoped}^2, \quad (2)$$

and the breakdown condition is given by

$$\frac{\alpha_1}{\alpha_1-\beta_1} - \frac{\beta_1}{\alpha_1-\beta_1}\exp\left[x_d(\alpha_1-\beta_1)\right] = \int_{F'_{heter}}^{F_{end}} \alpha_2(F)\exp\left[\int_{F'_{heter}}^{F}(\beta_2-\alpha_2)\frac{dF'}{dF/dx}\right]\frac{dF}{dF/dx}. \quad (3)$$

Here, ε_1 and ε_2 are the relative dielectric constants for InP and InGaAs, and have values of 12.3 and 12.9 respectively. ε_0 is the dielectric constant of vacuum and q is the electron charge. N_D is the unintentional doping concentration in the InGaAs absorption layer. σ_{InGaAs} ($=t_{InGaAs}N_{InGaAs}$) is the charge sheet density of the thin doped InGaAs layer. The remaining terms are shown in Fig. 1 and their values are listed in Table 1. In eqn. (3), α_1 and β_1 are impact ionization coefficients for electrons and holes in InP (at F_{br}), respectively, and α_2 and β_2 for InGaAs. F'_{heter} and F_{end} are the electric fields at breakdown at the top and the bottom of InGaAs absorption layer, respectively. If the ionization in the InGaAs absorption layer is ignored, then the right hand side of eqn. (3) is zero. dF/dx is the spatial gradient of the electric field in the absorption layer, and is $qN_D/\varepsilon_2\varepsilon_0$. In this work, Osaka's values are used for α_1 and β_1 [5], and Pearsall's values for α_2 and β_2 [6]. The unknown variables F_{br}, σ_{charge} and x_d can be found iteratively with experimental values of V_{mesa} and V_{br} as sole input parameters.

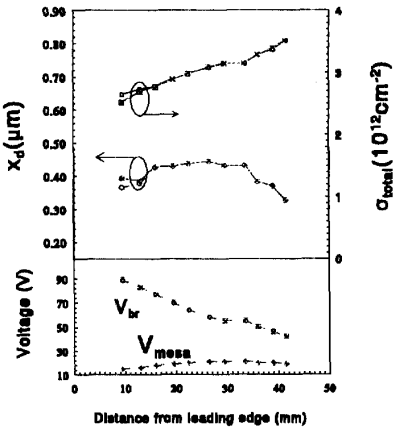

Fig. 3 The experimental Vbr and Vmesa and calculated x_d and σ_{total} across an entire 2" wafer (P555). The solid squares and circles are calculated results with InP/InGaAs ionizations, and the open squares and circles are with InP only ionization.

This technique for extracting x_d and σ_{charge} has been verified with other reported independent measurements over wafer, and the result of one wafer is shown in Fig. 3 in which $\sigma_{total} = \sigma_{charge} + N_G t_G + \sigma_{InGaAs}$.

Temperature dependence of V_{br}

The above procedure ensures a perfect match of V_{br} at room temperature. The temperature dependence of breakdown voltage is mainly due to the temperature dependence of α_1 and β_1, thus an analytical expression for α_1 and β_1 is much more convenient to model the temperature dependence of V_{br}. The empirical expressions used here for α_1 and β_1 [6] is

$$\alpha, \beta = \frac{qF}{E_i}\exp\left\{R - \sqrt{R^2 + \left[\frac{E_i}{qF\lambda}\right]^2}\right\} \quad (4)$$

with

$$R = 0.217\left(\frac{E_i}{E_r}\right)^{1.14} \quad (5)$$

Table 2 The values for the parameters of the impact ionization coefficients in InP at 300 K.

	E_i (eV)	E_r (meV)	λ (Å)
α_1	1.49	33.7	27.0
β_1	1.46	42.9	33.1

Table 3 The extracted x_d and σ for three typical APDs from a same wafer (P623) along with their experimental V_{mesa}, V_{br} at 20 °C.

	APD14	APD32	APD34
V_{mesa} (V)	25.8	24.8	20.6
V_{br} (V) @20 °C	45.3	55.8	69.3
x_d (μm)	0.551	0.572	0.502
σ (10^{12}cm^{-2})	2.659	2.466	2.175

and the temperature dependence of E_r and λ [7] is given by

$$E_r = E_{ro}\tanh(E_{ro}/2kT), \qquad \lambda = \lambda_o \tanh(E_{ro}/2kT). \qquad (6)$$

This temperature dependence can accurately describe impact ionization coefficients in Si and GaAs at different temperatures. F is the electric field, E_i is the ionization threshold energy, E_r is the average energy loss per phonon scattered, λ is the mean free path for optical phonon scattering, and E_{ro} and λ_o are the values of E_r and λ at 0 K. Furthermore, the temperature dependence of E_i can be assumed to be the same as the temperature dependence of the bandgap energy. Except for E_i, the parameters at 300 K for α_1 and β_1 listed in Table 2 are from Ref. [9]. The values for E_i are decreased by less than 10% to best fit Osaka's room temperature α_1 and β_1 [5] within the electric field range from 40 to 60 V/μm. This falls within the range used here and ensures consistency with our previous work [4].

Results and discussions

Three typical APDs from a same wafer (P623) with different V_{br} at room temperature will be discussed. The extracted x_d and σ_{charge} for these APDs are listed in Table 3 (V_{mesa} changes very little with temperature). The extracted x_d does not change significantly for APDs with different V_{br}, whereas the σ_{charge} decreases noticeably with an increase in V_{br}.

A typical (APD32) dark current versus bias voltage at different temperatures is shown in Fig. 4. The experimental V_{br} is defined as the voltage at which a DC current of 10 μA flows. The experimental V_{br} for the three APDs as function of temperatures $V_{br}(T)$ from -40 °C to 110 °C are shown as symbols in Fig. 5. It has been experimentally found and theoretically proven [10] that $V_{br}(T)$ for p^+-n Si APDs can be approximated by the linear expression $V_{br}(T) = V_{br}(T_o)[1+\beta(T-T_o)]$ with

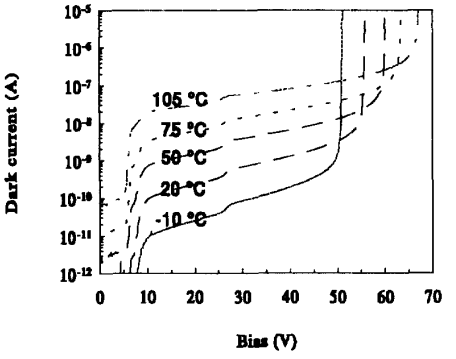

Fig. 4 A typical (APD32) dark current versus bias voltage at different temperatures.

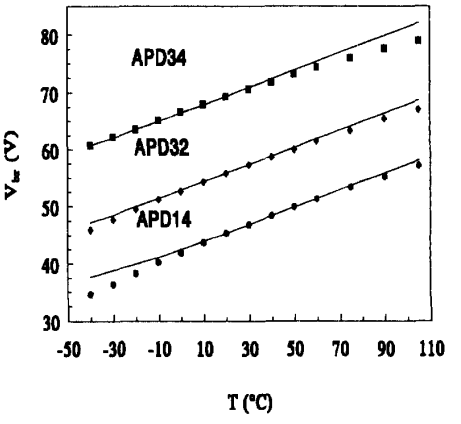

Fig. 5 The breakdown voltage V_{br} as function of temperature from -40 °C to 110 °C for three APDs. The symbols are experimental data, and the solid lines are theoretical calculations.

T in °C, and T_o, a reference temperature. Later on, it has been found experimentally that this expression can also be used empirically for p^+-n InP-based APDs [9, 11-12]. However, this expression is not appropriate for SAGCM APDs since β would change 100% from APD14 to APD34. This is because this expression was derived for abrupt p^+-n junctions [10], which have very high F_{br}. We found that a better empirical expression for breakdown voltage $V_{br}(T)$ at temperature T [4] is given by

$$V_{br}(T) = V_{br}(T_o) + \eta(T - T_o). \qquad (7)$$

where η is the temperature coefficient of V_{br}. The parameter η depends strongly on the semiconductor properties, but weakly on device parameters.

We will now use our physical model to calculate $V_{br}(T)$. The $V_{br}(T)$ calculated from the physical model (eqns. (2)

and (3)) for each APD are shown as solid lines in Fig. 5. The non-linearity at lower temperatures for APD14 is due to the un-depleted absorption region. However, disregarding this, the theoretical calculations are in good agreement to the experimental data, particularly between -20 °C to 70 °C for all three APDs. These results prove physically that the breakdown voltage due to avalanche breakdown is almost a linear function of temperature in SAGCM InP/InGaAs APDs, with a positive theoretical temperature coefficient η_{th}. For these particular APDs, the η_{th} does not change significantly from device to device, with a value of 0.148±0.002 V/°C at about 20 °C.

The deviation between the theoretical and experimental $V_{br}(T)$ at higher temperatures, particularly for APD34, indicates that the temperature dependence of α_1 and β_1 (which has not been verified experimentally before), needs to be modified at higher temperatures. Another set of parameters for eqn. (4) has been reported before [13], and preliminary results indicate that with this set of parameters, we can match the experimental data at higher temperatures, but not at lower temperatures. It seems that α_1 and β_1 with a combination of these two sets of parameters for eqn. (4) are better, at least as far as temperature dependence is concerned.

It is interesting to make comparisons to other types of InP/InGaAs APDs. For example, there are reported η values for InP p-n diodes of 0.144 V/°C [11] and 0.072 V/°C [9], for SAM InP/InGaAs APD of 0.14 and 0.18 V/°C [11], and 0.15 V/°C [12] at about 300 K. For the p-n diodes with η of 0.072 V/°C, the n side is relatively heavily doped with doping concentration $4x10^{16}$ cm^{-3} so that F_{br} is higher. For the others, their doping concentrations are smaller than $1x10^{16}$ cm^{-3}, and η values are between 0.14 to 0.18 V/°C. If the experimental V_{br} at lower temperatures for our APDs are linearly fitted, η is found to be distributed between 0.14 to 0.18 V/°C, too. However, our present model does not account for this small but discernible variation of η. The most likely reason for this incompleteness is the neglect of the ionization in the InGaAs absorption layer.

Finally, to our best knowledge, this is the first report of theoretical modelling of the temperature dependence of the breakdown voltage in any type of InP-based APDs. The empirical temperature dependence of the ionization coefficients used in this report represents their first verification, which will be very useful in modelling temperature dependence of other characteristics in InP-based APDs in the future.

In conclusion, we have developed a physical model to successfully interpret the temperature dependence of breakdown voltage in SAGCM InP/InGaAs APDs. The numerical results demonstrated that the breakdown voltages vary approximately as a linear function of temperature for the devices designed with a range of device parameters. The good agreement between the experimental and calculated V_{br} values at different temperatures implies that we have verified the empirical formula for temperature dependence of the impact ionization coefficients in InP.

Acknowledgments

We greatly acknowledge the technical help from D. McGhan, T. Baird (Northern Telecom Ltd.), D. G. Knight, R. Bruce, and other members of the Advanced Technology Laboratory of Bell-Northern Research. This research was partially supported by NSERC of Canada.

References

[1] L. E. Tarof et al., "Planar InP/InGaAs avalanche photodiodes with partial charge sheet in device periphery," *Appl. Phys. Lett.*, Vol. 57, pp. 670-672, 1990; L. E. Tarof et al., "High frequency performance of separate absorption grading, charge, and multiplication InP/InGaAs avalanche photodiodes," *IEEE Photon. Technol. Lett.*, PTL-5, pp. 672-674, 1993.

[2] M. Ito, T. Mikawa and O. Wada, "Optimum design of δ-doped InGaAs avalanche photodiode by using quasi-ionization rates," *IEEE J. Lightwave Technol.*, Vol. LT-4, pp. 1046-1050, 1991.

[3] R. Kuchibholta and J. C. Campell, "Delta-doped avalanche photodiodes for high bit-rate lightwave receivers,", *IEEE J. Lightwave Technol.*, Vol. LT-5, pp. 900-905, 1991.

[4] C. L. F. Ma, M. J. Deen, and L. E. Tarof, "A fast and accurate method of extracting two critical device parameters of separate absorption grading, charge, and multiplication InP/InGaAs avalanche photodiodes," *Proc. 24th European Solid State Device Research Conf.*, pp. 459-462, 1994.

[5] F. Osaka and T. Mikawa, "Excess noise design of InP/InGaAsP/InGaAs avalanche photodiodes," *IEEE J. Quan. Electron.*, Vol. QE-22, pp. 471-478, 1986.

[6] T. P. Pearsall, "Impact ionization rates for electrons and holes in GaInAs,", *Appl. Phys. Lett.*, Vol. 36, pp. 218-220, 1980.

[7] Y. Okuto and C. R. Crowell, "Energy-conservation considerations in the characterization of impact ionization in semiconductors," *Phys. Rev.*, Vol. 6, pp. 3076-3081, 1972.

[8] C. R. Crowell and S. M. Sze, "Temperature dependence of avalanche multiplication in semiconductors," *Appl. Phys. Lett.*, Vol. 9, pp. 242-244, 1966.

[9] Y. Takanashi and Y. Horikoshi, "Temperature dependence of ionization coefficients for InP and 1.3 μm InGaAsP avalanche photodiodes," *Jpn. J. Appl. Phys.*, Vol. 20, pp. 1907-1913, 1981.

[10] M. S. Tyagi, "Zener and avalanche breakdown in silicon alloyed p-n junctions," *Solid-State Electron.*, Vol. 11, pp. 99-128, 1968.

[11] N. Susa, H. Nakagome, H. Ando, and H. Kanbe, "Characteristics in InGaAs/InP avalanche photodiodes with separated absorption and multiplication regions," *IEEE J. Quan. Electron.*, Vol. QE-17, pp. 243-250, 1981.

[12] S. R. Forrest and O. K. Kim, "Analysis of the dark current and photoresponse of InGaAs/InP avalanche photodiodes," *Solid-State Electron.*, Vol. 26, pp. 951-968, 1983.

[13] H. F. Chau and D. Pavlidis, "A physics-based fitting and extrapolation method for measured impact ionization coefficients in III-V semiconductors," *J. Appl. Phys.*, Vol. 72, pp. 531-538, 1992.